A Numerical Method for Electrical Potential on Membranes with Fixed Charge

Y. Sun and L. Song[1]

Department of Civil, Environmental, and Construction Engineering

Texas Tech University

Lubbock, TX 79409

1 Corresponding author

ABSTRACT

The potential developed on a membrane with fixed charge plays crucial roles in many biological and engineering systems. The classic Teorell-Meyer-Siever (TMS) theory gives an analytical expression of the membrane potential only for limited cases of simple solutions. A numerical method that can be applied to the general cases was developed in this study. With a boundary updating scheme, a numerical solution to the Nernst-Planck-Poisson equations was obtained rigorously without the commonly used simplifications and assumptions in previous studies. The features of the membrane potentials with different fixed charges were investigated with this numerical method under various conditions. The validity of this numerical method was verified by identical values of Donnan potential obtained with well-established analytical methods. The suitability and applicability of analytical TMS model were assessed by comparison to the numerical method.

KEY WORDS

Membrane potential, Nernst-Planck-Poisson equations, Teorell-Meyer-Siever model, Donnan potential, numerical modeling, boundary updating scheme.

1. Introduction

When a permselective membrane separates two electrolyte solutions of difference composition or concentration, an electrical potential usually develops on the membrane, which can be a result of differential diffusion of cations and anions [1, 2], Donnan effect of the fixed charge on the membrane [3, 4], or both [5, 6]. Membrane potential plays an important role in many biological and engineering systems, such as signal generation and transmission in neural system [7-9], proton transport in fuel cell [10], and desalination in electrodialysis [11, 12]. It was recently reported that the change of membrane potential beyond its normal range could be used to diagnose cancers from normal cells [13-15]. Therefore, it is paramount importance to develop the methods that can determine the membrane potential accurately.

Development of potential on a membrane is a very complex phenomenon involves many processes, such as convection of liquid, differential diffusion of ions, electrostatic draft of ions, and more. The magnitude of membrane potential is also affected by the properties of membrane and solutions. Although it is well established that the membrane potential is governed by Poisson equation coupled with the Nernst-Planck equation for the ion concentration distribution along the membrane thickness, the analytical expression of the classic Teorell-Meyer-Siever (TMS) model is only applicable to a few special cases with simple solutions [3, 16, 17]. It remains a serious challenge to quantify the membrane potential for more general cases [18, 19].

An optional method for the membrane potential is to seek numerical solutions of the coupled Nernst-Planck and Poisson (NPP) equations directly. Usually, when a numerical solution of governing equations is pursued, it is preferred to do it rigorously without making simplifications or assumptions. However, most of the reported numerical methods of NPP equations were obtained with some unreasonable assumption of boundary conditions [20-22].

The single standing-out obstacle for more rigorous form of numerical solutions is the setup of the appropriate boundary conditions of potential and ion concentration at the membrane surfaces [2, 23]. The potentials and ion concentrations at the boundaries cannot be assigned easily because they are interdependent and must satisfy certain relationship, which can only be known after solution of NPP equations is obtained. But the boundary conditions are required before the solution procedure can be started. This deadlock is the main reason for the use of the unrealistic assumptions (e.g., electroneutrality) in the numerical solution procedures.

The recently reported boundary updating scheme [24] is a numerical method that can handle the boundary conditions of NPP equations rigorously. With this scheme, the NPP equations can be solved numerically under the true boundary conditions pertinent to the realistic problems. It was demonstrated that the scheme worked well for the membranes of no-fixed-charge. The numerical solution was verified with the analytical solution when it was applied to the simplified case, from which the analytical solution was derived. The new numerical method for the first time was able to reveal the true features of ion transport and membrane potential without using unrealistic assumptions to distort the problem.

The main objective of this current paper is to apply the boundary updating scheme to study numerically the potential developed on the membranes with fixed charge. The numerical solutions of NPP equations for the membranes with various levels of fixed charge were obtained and the suitability and accuracy of the numerical method were discussed. The impact of membrane fixed charge on the membrane potential and potential components were studied. Finally, the TMS model was compared and assessed with the numerical method for its applicability and limitations.

2. Materials and Methods

2.1. *Governing equations*

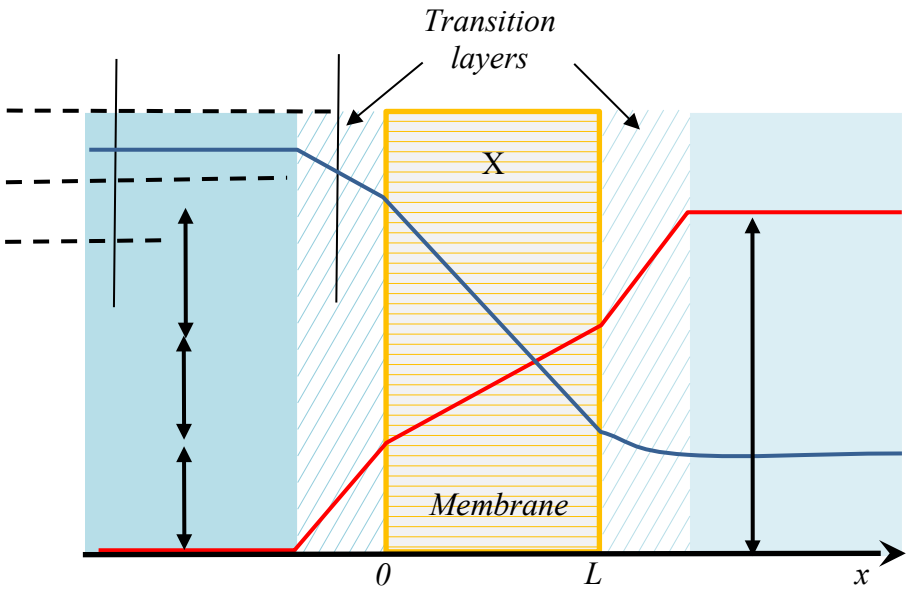

Fig. 1. Schematic of ion transport across a membrane with fixed charge

The problem under consideration is to determine the membrane potential at steady state as schematically shown in Fig. 1. A permselective membrane of fixed charge X separates two solutions of concentration C_{b0} and C_{bL}, respectively. There is a transition layer on each side of the membrane between the membrane surface and the bulk solution. While electroneutrality is always maintained in the bulk solutions, charge is usually unbalanced in transition layers because the attraction of counter-ions and repulsion of co-ions by the charge on the membrane. As a result, both ion concentrations and potential on the membrane surfaces differ from those in the bulk solutions, as schematically described by the lines for concentrations and potential in Fig. 1.

The ion concentrations and potential on a membrane are governed by the coupled Nernst-Planck and Poisson (NPP) equations,

$$\frac{dC_i}{dt} = D_i \frac{d^2 C_i}{dx^2} + \frac{D_i z_i F}{RT} \frac{d}{dx}\left(\frac{d\psi}{dx} C_i\right) \quad (1)$$

$$\frac{d^2\psi}{dx^2} = \frac{-F}{\epsilon}\left(X + \sum_i z_i C_i\right) \quad (2)$$

where C_i is the concentration of ion i, D_i is the diffusion coefficient of ion i, x is the spatial coordinate perpendicular to the membrane, z_i is the valance of ion i, F is the Faraday constant, R is the gas constant, ψ is the potential, X is the density of the fixed charge, and ϵ is the dielectric constant of the membrane material.

One challenging issue for the solution of the NPP equations is that there is usually not sufficient information to specify the appropriate boundary conditions. The reasons are that the ion concentrations and potential on the boundaries (membrane surfaces) are related to each other and that the relationship cannot be known before the equations have been solved. The unsteady state Nernst-Planck equation is used for the steady state problem because it helps to handle the boundary conditions effectively.

2.2. Boundary updating scheme

The boundary updating scheme was developed to overcome the difficulty in specifying the boundary conditions for the NPP equations at steady state. The scheme starts with a known state of boundaries of the membrane. For example, with an initially neutral membrane, there is no potential on the membrane (referring to the bulk solutions) and the ion concentrations at the boundaries (on the membrane surfaces) are equal to the bulk solutions, i.e.

$$C_{i0} = C_{ib0} \quad (3)$$

$$C_{iL} = C_{ibL} \quad (4)$$

$$\psi_0 = 0 \tag{5}$$

$$\left.\frac{d\psi}{dx}\right|_{x=L} = 0 \tag{6}$$

where $C_{i0}$and C_{iL} are the concentrations of ion i on the left surface and right surface of the membrane, respectively, C_{ib0} and C_{ibL} are the concentrations of ion i in the bulk solutions on the left and right sides of the membrane, respectively, and ψ_0 is the potential on the left surface of the membrane, and $\left.\frac{d\psi}{dx}\right|_{x=L}$ is the derivative of membrane potential at the right surface of the membrane. The ion concentrations on the membrane surfaces equal to the bulk solutions because there are not electrical forces on the neutral membrane to repel co-ions and to attract counter-ions.

The governing equations Eqs. (1) and (2) with boundary conditions Eqs. (3) - (6) completely define the membrane transport problem and can be solved with common numerical methods, e.g., Crank-Nicolson method for Nernst-Planck equation and central difference for Poisson equation. From the numerical solutions, the ion fluxes at the two boundaries can be determined,

$$J_i\big|_{0 \vee L} = -D_i\left(\frac{d\,C_i}{dx} + \frac{F}{RT}\frac{d\psi}{dx} z_i C_i\right)\Bigg|_{0 \vee L} \tag{7}$$

where J_i is the flux of ion i. The derivatives of concentration and potential at the two membrane surfaces are calculated from the numerical solutions.

The net charges in the two transition layers can be calculated with

$$Q_0 = Q_0^{'} - \sum_i F z_i J_i\big|_0 \Delta t \tag{8}$$

and

$$Q_L = Q_L^{'} + \sum_i F z_i J_i\big|_L \Delta t \tag{9}$$

where Q_0 and Q_L are the net charges in the transient layers on left and right sides of the membrane, respectively, $Q_0^{'}$ and $Q_L^{'}$ are the net charges at the previous time step in the transient layers on left and right sides of the membrane, respectively, and Δt is timestep. At the first timestep, $Q_0^{'} = 0$ and $Q_L^{'} = 0$ for an initially neutral membrane.

The boundary conditions at any timestep can be directly updated with the cumulative net charges by

$$C_{i0} = C_{ib0} e^{\frac{z_i F \lambda_0}{RT\epsilon} Q_0} \tag{10}$$

$$C_{iL} = C_{ibL} e^{\frac{z_i F \lambda_L}{RT\epsilon} Q_L} \tag{11}$$

$$\psi_0 = \frac{-\lambda_0}{\epsilon} Q_0 \tag{12}$$

$$\left.\frac{d\psi}{dx}\right|_{x=L} = \frac{1}{\epsilon} Q_L \tag{13}$$

where λ_0 and λ_L are the Debye lengths of the solutions on the left and right sides of the membrane, which are calculated by

$$\lambda_0 = \sqrt{\frac{\epsilon RT}{\sum_i F^2 z_i^{\,2} C_{ib0}}} \tag{14}$$

$$\lambda_L = \sqrt{\frac{\epsilon RT}{\sum_i F^2 z_i^2 C_{ibL}}} \tag{15}$$

Numerical solution of the NPP equation can be obtained for the next timestep with the updated boundary conditions. The above procedure can be repeated with the newly obtained numerical solution to update the boundary conditions for the next timestep until steady state, which is indicated by the null current condition,

$$\sum_i z_i J_i = 0 \tag{16}$$

With boundary updating scheme, the concentration boundary conditions are always consistent with potential boundary conditions at any time step. Therefore, the appropriate boundary conditions are guaranteed for the NPP equations at the steady state to ensure that the right numerical solution is obtained.

2.3. Calculation of membrane potentials

With the numerical solution at the steady state, the ion fluxes can be calculated by

$$J_i = -D_i\left(\frac{dC_i}{dx} + \frac{F}{RT}\frac{d\psi}{dx} z_i C_i\right) \tag{17}$$

The total membrane potential can be calculated with,

$$\psi_T = \Delta\psi_0 + \Delta\psi_m + \Delta\psi_L \tag{18}$$

where ψ_T is the total potential of the membrane, $\Delta\psi_m$ is the potential difference across the membrane, and $\Delta\psi_0$ and $\Delta\psi_L$ are the potential differences across the transition layers on the two sides of the membrane. The potential difference across the membrane thickness can be

determined from the numerical solution of the Poisson equation. The two potential differences across the transition layers can be calculated from the cumulated charge in the layers with

$$\Delta\psi_0 = \frac{-\lambda_0}{\epsilon} Q_0 \tag{19}$$

$$\Delta\psi_L = \frac{\lambda_L}{\epsilon} Q_L \tag{20}$$

3. Simulations and discussions

A C++ program of the numerical procedure described above was developed on Visual Studio 2019 for the study of potential on the membrane with fixed charged under various conditions. All simulations were done on a PC with CPU of Intel i7-9700 at 3.00Ghz. A numerical solution of the governing equations can be obtained in a few seconds. Unless other specified, the values of parameters used in the simulations are listed in Table 1.

Table 1 Default parameter values used in numerical simulations

Parameter	Symbol	Unit	Value
Membrane dielectric constant	ϵ	F/m	6.92×10^{-10}
Membrane thickness	L	m	5×10^{-8}
Temperature	T	K	298.15
Time step	Δt	s	10^{-9}
Number of spatial steps	N		1000
Number of ions			2
Valence of cation	z_+		+1
Valence of anion	z_-		-1
Diffusivity of cation	D_+	m^2/s	1×10^{-10}
Diffusivity of anion	D_-	m^2/s	2×10^{-10}
Fixed charge	X	mol/m^3	10
Concentration on the left side	C_{b0}	mol/m^3	10

Concentration on the right side	C_{bL}	mol/m^3	5

3.1. The effectiveness of boundary updating scheme

The numerical solution of NPP equations with the parameters of default values as given in Table 1 is presented in Fig. 2. The numerical solution for a membrane of no-fixed-charge with the same parameters is also shown as a comparison in the figure. It can be seen in Fig. 2a that both cation concentration and anion concentration at the membrane surfaces (boundaries) differ significantly from the bulk concentrations, which are 10 mol/m^3 and 5 mol/m^3, respectively, on the left and right sides of the membrane. The different cation and anion concentrations at the membrane surfaces are an essential feature of ion transport across the membrane. The boundary updating scheme can handle this feature of the boundary conditions effectively. The scheme is particularly suitable for the membranes of fixed charge because of bigger differences between cation and anion concentrations at the membrane surfaces than that for the membrane of no-fixed-charge.

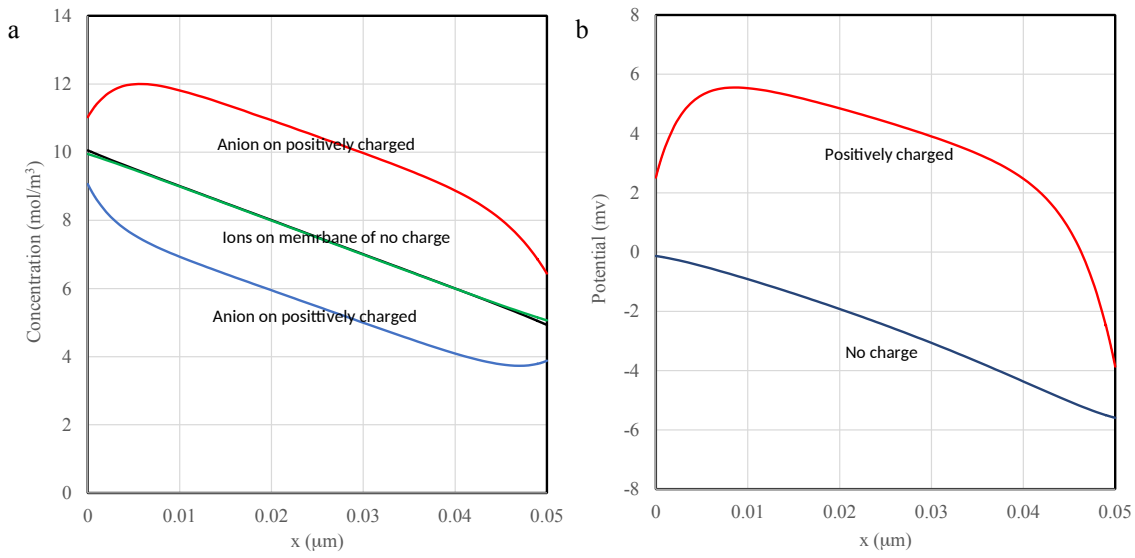

Fig. 2 (a) Concentration distributions and (b) potential distributions across the membrane thickness

The anion concentration is higher than the cation concentration throughout the entire membrane thickness because of the positive fixed charge on the membrane. It can be seen that the electroneutrality can only be maintained in the middle section of the membrane thickness, i.e., the difference between anion concentration and cation concentration is roughly equal to the fixed charge carried by the membrane. The lower anion concentrations and higher cation concentrations near the membrane surfaces are the results of ion transfer between the membrane and solutions. The distributions of ions for the membrane of no-fixed-charge are relatively simple. The concentrations of anions and cations equal to each other almost through the entire membrane thickness with exceptions in the narrow regions near the two membrane surfaces. The details of the concentration difference cannot be seen clearly in the lines for ion concentrations on the membrane of no-fixed-charge. In fact, the anion is lower in the region at the left side but higher at the right side. Interested readers can find more details about the ion concentration distributions on the membrane of no-fixed-charge in our previous paper [24].

The corresponding potential distributions are presented in Fig 2b. The potential of the membrane of no-fixed- charge decreases monotonically from the left surface to the right surface because of the higher mobility of the anions. The potential of the membrane of positive fixed charge changes more complexly than that of no-fixed- charge. The middle section of the charged membrane declines with a rate similar to the membrane of no-fixed- charge. The variation of potential is obviously due to differential diffusion of ions with different mobilities. There is a jump in an initial region and a drop in the final region of the potential for the membrane of fixed charge. These variations are because of the repulsion of the co-ions and attraction of counter-ions by the fixed charge of the membrane, i.e. the Donnan effect of the fixed charge. The

potentials at the membrane surfaces were again generated by the boundary updating scheme, which are intimately corelated to the ion concentrations at the membrane surfaces. Such rigorous numerical solutions of NPP equation with the well-defined consistent boundary conditions have not been obtained with any method other than the boundary updating scheme.

3.2. Impact of the fixed charge

The potential distributions along the membrane thickness at different fixed charges are presented in Fig. 3. The line in the middle presents the potential profile for the membrane of no-fixed-charge. The potentials for the positively charged membranes are all above the line of the uncharged membrane while the negatively charged membranes have potentials are below that of the uncharged membrane. This feature can be attributed to the Donnan effect of the fixed charge. The middle sections of all the potential lines decline from the left to the right with about the same rate, which reflects the impact of differential diffusion of cations and anions on the potential profiles.

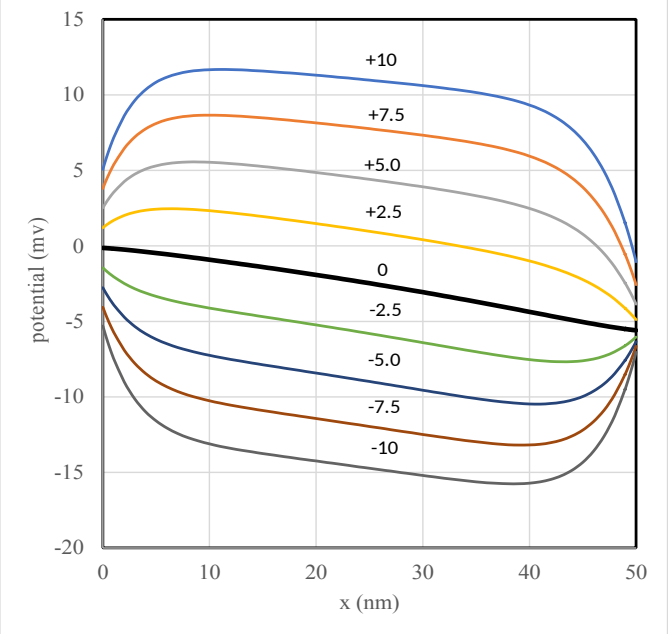

Fig. 3 Potential distributions across the membrane thickness for membranes with different fixed charge. The charge density is indicated on the lines.

An interesting and useful feature of the boundary updating scheme is that the potential differences across the transition layers can be determined simultaneously with the numerical solution of the NPP equations. The potential differences across the transition layers can be relatively large for the membranes with fixed charge. The potential differences across the two transition layers and across the membrane are presented in Fig. 4, together with the total membrane potential, which is the summation of all the three potential components. It can be seen that the variation of potential difference across the membrane $\Delta\varphi_m$ is the smallest (~5mv) under the simulation conditions. The potential difference across the left transition layer $\Delta\varphi_0$ varies in a range that is more than doubled the range for the membrane potential (~ 10 mv). The potential difference across the right transition layer $\Delta\varphi_L$ varies the largest in a range of about 25 mv. Under the simulation conditions, the potentials in the transition layers are primarily controlled by Donnan potential. The larger absolute value of the potential difference in the right transition layer is reasonable because the Donnan potential for the same fixed charge is greater for the lower solution concentration. The total potential difference of the membrane $\Delta\varphi_T$ decreases monotonically throughout the entire range of fixed charge.

The ion fluxes at various fixed charge are listed in Table 2 with corresponding potential differences across the membrane and the total membrane potentials. The impact of the fixed charge on flux is much smaller than on the potentials. For the given range of fixed charge used in the simulations, the maximum change in flux is smaller than 50%. It clearly demonstrates that the ion flux through the membrane is largely determined by the concentration difference across the membrane, which is constant at 5 mol/m^3 for all fixed charges.

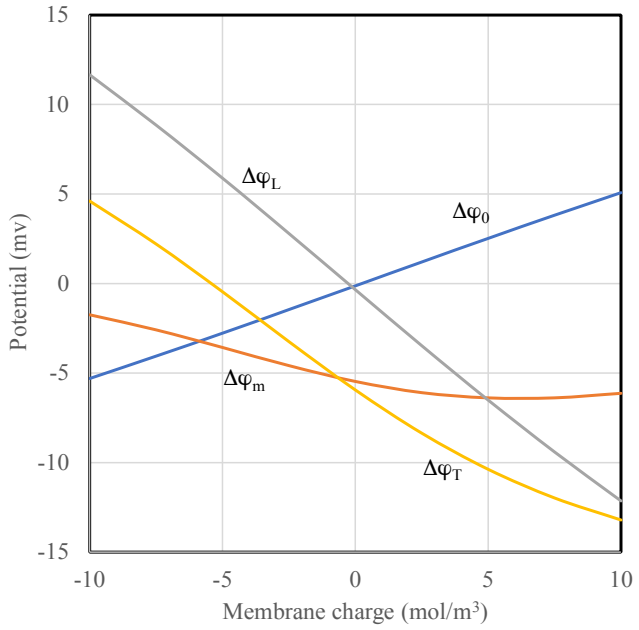

Fig. 4 Total membrane potential and potential components

Table 2 Potentials and ion fluxes at different fixed charge

Charge (mol/m^3)	$\Delta\varphi_m$ (mv)	$\Delta\varphi_T$ (mv)	Flux (mol/m^2.s)
-10.00	-1.74	4.61	1.36×10^{-2}
-7.50	-2.58	2.21	1.40×10^{-2}
-5.00	-3.57	-0.45	1.41×10^{-2}
-2.50	-4.58	-3.24	1.39×10^{-2}
0.00	-5.46	-5.94	1.33×10^{-2}
2.50	-6.09	-8.36	1.25×10^{-2}
5.00	-6.38	-10.37	1.15×10^{-2}
7.50	-6.38	-11.97	1.05×10^{-2}
10.00	-6.13	-13.20	9.55×10^{-3}

Ion flux is seen to decrease monotonically with the increasing positive fixed charge. However, ion flux increases initially and then decreases with increasing negative fixed charge.

In this particular example, the cations are the limiting factor for ion transport because they have smaller mobility than the anions. The positive fixed charge will reduce cation concentration in the membrane and therefore further reduce the capacity of ion transport. On the other hand, the negative fixed charge of the membrane can increase cation concentration in the membrane so that the capacity of ion transport can be increased. Of cause, the anion concentration would be reduced by the negative fixed charge. Because of the larger mobility of anions, the impact on ion flux by the reduced anion concentration in a certain range would be over-compensated by the benefit of the increased cation. Beyond the concentration range, the anion would become the limiting factor for ion transport. Further reduction of the anion would reduce the ion flux. As shown in Table 2, the ion flux obtains the highest value at the fixed charge of -5 mol/m^3.

3.3. Donnan potential

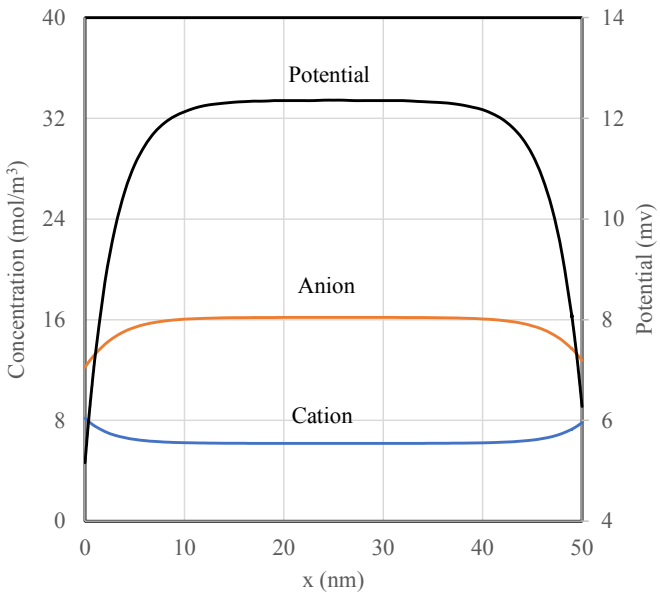

Fig. 5 Distributions of cation and anion concentration and potential for equal solution concentration on both sides of the membrane.

As a demonstration of the boundary updating scheme, the Donnan potential was calculated by solving the NPP equations with equal solution concentrations on both sides of the membrane. The concentration and potential distributions from a numerical solution is presented in Fig. 5. The concentrations $C_{b0} = C_{bL} = 10$ mol/m^3 and positive fixed charge $X = 10$ mol/m^3 were used in the simulation. It can be seen that anion concentration is higher than cation concentration throughout the membrane thickness because of the positive fixed positive charge on the membrane. In the middle section of the membrane thickness (~10-40nm), the electroneutrality is basically satisfied because difference between anions and cations, which is about 10 mol/m^3, equals to the fixed charge on the membrane. Lower anion concentration and higher cation concentration were observed in regions near the membrane surfaces as a result of ion exchanges with the solutions. This unbalanced charge is actually the cause of Donnan potential. The boundary updating scheme is able to set up the appropriate boundary conditions of ion concentration and potential at membrane surfaces for the NPP equations to determine the Donnan potential.

The potential distribution is also presented in Fig. 5 for a positively charged membrane. The potential increases from the membrane surface to the middle of the membrane. The value of the plateau of the potential curve is the Donnan potential, which is 12.36 mv in this case. A well-established formula for the Donnan potential is [3, 4]

$$\Delta\psi_D = \frac{RT}{F}\ln\left[\frac{1}{2C}\left(X+\sqrt{X^2+4C^2}\right)\right] \qquad (21)$$

where $\Delta\psi_D$ is the Donnan potential and C is the concentration of 1-1 electrolyte solution. The derivation of Eq. (21) was obtained with the electroneutrality assumption that positive charge

and negative charge are equal to each other inside of the membrane. The Donnan potentials determined with the two different methods are presented in Table 3. It is a good surprise to find that the two methods give identical values of the Donnan potentials up to 3 effective digits! It is a convincing evidence that the numerical method for the membrane potential is very accurate. At the same time, it also shows that the use of electroneutrality assumption to reach the analytical expression of the Donnan potential is acceptable though it is unphysical fundamentally.

Table 3 Analytically and numerically calculated Donnan potentials

X (mol/m^3)	Analytical	Numerical	Error (%)
-10.00	-12.363	-12.350	-0.105
-7.50	-9.422	-9.415	-0.070
-5.00	-6.358	-6.353	-0.074
-2.50	-3.203	-3.201	-0.066
2.50	3.203	3.201	-0.066
5.00	6.358	6.353	-0.074
7.50	9.422	9.415	-0.070
10.00	12.363	12.360	-0.024

3.4. Comparison of TMS model with numerical method

The membrane potential for the 1-1 electrolyte solution on both sides of a membrane can be calculated analytically with the TMS model:

$$\Delta\varphi = \frac{RT}{F}\ln\frac{C_{bL}}{C_{b0}}\frac{\sqrt{X^2+4C_{b0}{}^2}+X}{\sqrt{X^2+4C_{bL}{}^2}+X} - \frac{RT}{F}U\ln\frac{\sqrt{X^2+4C_{bL}{}^2}+UX}{\sqrt{X^2+4C_{b0}{}^2}+UX} \qquad (22)$$

where U is the mobility coefficient that is defined as

$$U = D_{+¿} - \frac{D_{-¿}}{D_{+¿} + D_{-¿}} ¿ \quad (23)$$

where $D_{+¿¿}$ and $D_{-¿¿}$ are the diffusion coefficient of cations and anions, respectively. The membrane potentials calculated analytically with Eq. (22) for various mobility coefficients ware presented (as dots) in Fig. 6. In the calculation, concentrations $C_{b0} = 10$ mol/m^3 *and* $C_{bL} = 1$ mol/ m^3 were employed on two sides of the membrane. The numerically calculated membrane potentials for the same conditions were also plotted (as lines) in Fig. 6.

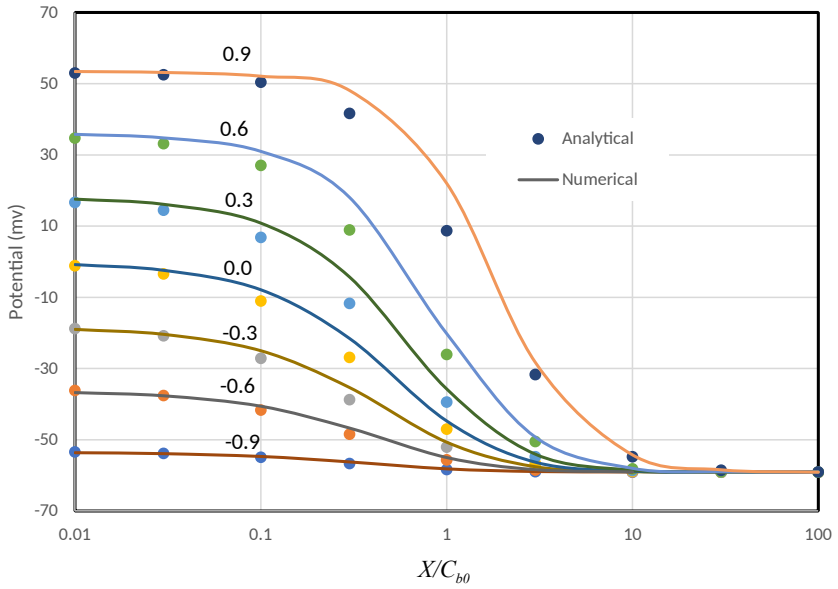

Fig. 6 Membrane potentials calculated analytically (symbols) and numerically (lines) as a function of the ratio of fixed charge to salt concentration on the right side of the membrane. The mobility coefficients are indicated on the graphs.

It can be seen that the membrane potentials calculated analytically with TMS model agree well with the values calculated numerically when the ratio of X/C_{b0} is smaller than 0.03 or greater than 30. There are significant discrepancies between the two membrane potentials in the range of $0.03 < X/C_{b0} < 30$. The analytical calculated values are systematically lower than the true membrane potentials, with the biggest discrepancy at $X/C_{b0} = 1$. For example, the analytical

value (8.71mV) is only about 40% of the numerically determined membrane potential (22.0mV) for mobility coefficient of 0.9 at this point.

The TMS model is not a rigorous solution of the governing equations because it is simply impossible. The assumptions and simplifications (5, 6) that are used in the process to reach the analytical solution bring certain divergence from the true solution at the same time. The numerical calculated membrane potentials can be taken as the true values because no assumptions and simplifications are made in the process to seek the solution of the governing equations. Furthermore, the analytical TMS model can be only used for limited cases with two ions of equal charge in solutions while the numerical methods can be applied to the general cases with multiple ions of various charges.

4. Conclusions

The potential of a membrane with fixed charge can be rigorously investigated numerically with the boundary updating scheme. The numerical method can not only determine the total membrane potential, but also the potential differences across the transition layers and across the membrane. The detailed distributions of ion concentrations and potential along the membrane thickness reveal the fundamental mechanism for the development of membrane potentials. The well-matched values of Donnan potentials determined separately with analytical method and numerical method can be a strong support to the validity and accuracy of the numerical method. It has been demonstrated that the analytical TMS model tends to predict lower membrane potentials systematically, especially for the membranes with intermediate range of fixed charge. The numerical method can not only be more accurate than the analytical TMS model for special cases but also be applicable to the general cases for which the analytical model is not applicable.

Author Contributions

L.S. developed the theory and designed the framework of this simulation study, interpreted the results, and wrote the manuscript. Y.S. performed and analyzed the simulations and calculations, interpreted the results, and co-wrote the manuscript. All authors provided feedback on the manuscript.

Acknowledgments

The authors acknowledge partial support of Bureau of Reclamation through the Grant R17AC00140.

References

[1] J. Hirvonen, L. Murtomaki, K. Kontturi, Effect of diffusion potential, osmosis and ion-exchange on transdermal drug delivery: theory and experiments, J. Control. Release. 56 (1998) 33-39.

[2] R. Filipek, K. Szyszkiewicz-Warzecha, B. Bożek, M. Danielewski, A. Lewenstam, Diffusion Transport in Electrochemical Systems: A New Approach to Determining of the Membrane Potential at Steady State. Defect and Diffusion Forum 283-286 (2009) 487-493.

[3] O Sten-Knudsen, Biological Membranes: Theory of Transport, Potentials and Electric Impulses, Cambridge University Press, 2002.

[4] A.H. Galama, J.W. Post, M.A. Cohen Stuart, P.M. Biesheuvel, Validity of the Boltzmann equation to describe Donnan equilibrium at the membrane–solution interface, J. Membr. Sci. 442 (2013) 131–139.

[5] T. Teorell, An Attempt to Formulate a Quantitative Theory of Membrane Permeability. *Proc. Soc. Exp. Biol. Med.* 33 (1935) 282–285.

[6] G.B. Westermann−Clark, C. Christoforou, The exclusion-diffusion potential in charged porous membranes, *J. Electroanal. Chem.* 198 (1986) 213-231.

[7] S. Oh, C. Fang-Yen, W. Choi, Z. Yaqoob, D. Fu, Y. Park, R. R. Dassari, M. S. Feld, Label-free imaging of membrane potential using membrane electromotility, Biophys. J. 103 (2012) 11–18.

[8] R. C. Scaduto, L. W. Grotyohann, Measurement of Mitochondrial Membrane Potential Using Fluorescent Rhodamine Derivatives, Biophys. J. 76 (1999) 469–477.

[9] BenoTt Roux, Influence of the Membrane Potential on the Free Energy of an Intrinsic Protein, Biophys. J. 73 (1997) 2980-2989.

[10] H. Strathmann, Electrodialysis, a mature technology with a multitude of new applications, Desalination 264 (2010), 268-288.

[11] V. Nikonenko, V. Zabolotsky, C. Larchet, B. Auclair, G. Pourcelly, Mathematical description of ion transport in membrane systems. Desalination 147 (2002) 369-374.

[12] M. Levin, Molecular bioelectricity in developmental biology: new tools and recent discoveries, Bioessays 34 (2012) 205-217.

[13] M. Yang, W.J. Brackenbury, Membrane potential and cancer progression, Front Physiol. 4 (2013) 185.

[14] L. Pardo, C. Contreras-Jurado, M. Zientkowska, F. Alves, W. Stühmer, Role of voltage-gated potassium channels in cancer, J Membrane Biol. 205 (2005) 115-124.

[15] E. J. F. Dickinson, L. Freitag, R. G. Compton, Dynamic theory of liquid junction potentials. J. Phys. Chem. B 114 (2010) 187-197.

[16] A. L. Hodgkin, B. Katz, The effect of sodium ions on the electrical activity of the giant axon of the squid. J. Physiol. 108 (1949) 37-77.

[17] S. W. Feldberg, On the dilemma of the use of the electroneutrality constraint in electrochemical calculations. Electrochem. Commun. 2 (2000) 453–456.

[18] A. Syganow, E. von Kitzing, (In)validity of the constant field and constant currents assumptions in theories of ion transport. Biophys. J. 76 (1999) 768–781.

[19] M. Kato, Numerical Analysis of the Nernst-Planck-Poisson System. J. theor. Biol. 177 (1995) 299-304

[20] M. Blank, The surface compartment model: a theory of ion transport focused on ionic processes in the electrical double layers at membrane protein surfaces. Biochimica et Biophysica Acta 906 (1987) 277-294.

[21] R. P. Buck, Kinetics of bulk and interfacial ionic motion: microscopic bases and limits for the Nernst-Planck equation applied to membrane systems. J. Membr. Sci. 17 (1984) l-62.

[22] J. W. Perrama, P. J. Stiles, On the nature of liquid junction and membrane potentials. Phys. Chem. Chem. Phys. 8 (2006) 4200-4213.

[23] Y Sun, L Song, On rigorous definition of ion transport process and accurate determination of membrane potential at steady state, AIChE J. 65 (2019) e16715.